ACS Catalysis

Research Article

pubs.acs.org/acscatalysis

Generation of H_2O_2 and OH Radicals on Bi_2WO_6 for Phenol Degradation under Visible Light

Jiayi Sheng, Xiaojin Li, and Yiming Xu*

State Key Laboratory of Silicon Materials and Department of Chemistry, Zhejiang University, Hangzhou 310027, China

Supporting Information

ABSTRACT: In thermodynamics, the one-electron reduction of O_2 by the conduction band electrons of Bi_2WO_6 or WO_3 is not allowed. However, many studies have reported that Bi_2WO_6 is photocatalytically active for organic degradation in aerated aqueous suspension. In this work, the photocatalytic activities of Bi_2WO_6 and WO_3 under visible light have been compared by using phenol degradation as a model reaction. In aerated aqueous solution, Bi_2WO_6 and WO_3 were indeed active and inactive, respectively, as reported. However, by using Pt as a catalyst for O_2 reduction, or by using H_2O_2 as an electron scavenger, Bi_2WO_6 became much less active than WO_3. Similar results were also obtained in the production of H_2O_2 under visible light, and in the generation of $^{\bullet}OH$ radicals under UV light, measured by a spin-trapping electron paramagnetic resonance (EPR) spectroscopy. Moreover, in the presence of catalase to completely remove H_2O_2, the EPR signal due to $^{\bullet}OH$ radical was reduced, but not disappeared. These observations indicate that the irradiated Bi_2WO_6 is not only active for water oxidation to $^{\bullet}OH$ but also active for the two-electron reduction of O_2 to H_2O_2, the latter of which hardly occurs with the irradiated WO_3.

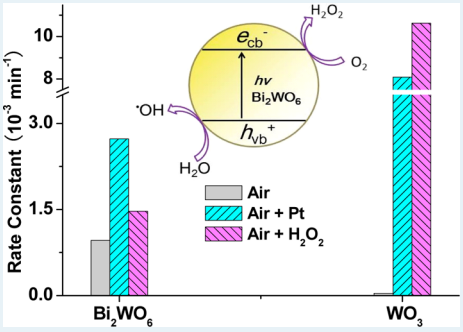

KEYWORDS: *Bi_2WO_6, platinization, EPR signal, flat band potential, two-electron reduction*

INTRODUCTION

Photocatalysis of TiO_2 for environmental remediation has been studied for over 30 years.[1−3] It is recognized that with the aid of O_2, H_2O and UV light, many organic pollutants over TiO_2 can degrade into CO_2, and/or small fragments at normal temperature and pressure. In those reactions, various reactive species are involved, including the conduction band electron (e_{cb}^-), the valence band hole (h_{vb}^+), superoxide radical ($O_2^{\bullet-}$), hydroxyl radical ($^{\bullet}OH$), and singlet oxygen ($^1O_2$). However, the UV light, required for the band gap excitation of TiO_2, is expensive and accounts for only a small part of sunlight reaching the Earth surface. Therefore, development of a visible-light-driven photocatalyst is an urgent task in this field.

In recent years, WO_3 and Bi_2WO_6, as visible light photocatalysts, have attracted much attention.[4−10] These semiconductors possess a small band gap energy, falling within the solar spectrum (about 2.6 eV for WO_3, and 2.8 eV for Bi_2WO_6). Importantly, their valence band holes have a potential reactivity similar to that of TiO_2 for water oxidation to $^{\bullet}OH$ radicals. Many studies have reported that Bi_2WO_6 is active for the photocatalytic degradation of acetic acid, rhodamine B (RhB) and methylene blue (MB) in aerated aqueous solution under UV or visible light.[11−19] However, for organic degradation in aerated aqueous suspensions, WO_3 is not active either under UV or visible light. The WO_3-photocatalyzed reaction is fast only in the presence of Pt or Pd as a cocatalyst,[4,5] or in the presence of H_2O_2 as an electron scavenger.[6,7] These additives of noble metals and H_2O_2 is costly to practical application. In this regard, Bi_2WO_6 is better than WO_3 as environmental photocatalysts, and thus it is worthy of being further studied.

The question arises why Bi_2WO_6 has a photocatalytic activity superior to that of WO_3. It have been reported that the conduction band edges (E_{CB}) for WO_3 and Bi_2WO_6 in aqueous solution are similar, which are approximately 0.30−0.80[7,8] and 0.20−0.57 V[15−17] versus normal hydrogen electrode (NHE) at pH 0, respectively. These values of E_{CB} are all more positive than the one-electron reduction potential of O_2 (E^o = −0.05 V vs NHE). Then, the one-electron reduction of O_2 by e_{cb}^- on WO_3 or on Bi_2WO_6 would be not allowed in thermodynamics. Because e_{cb}^- and h_{vb}^+ are formed in a pair, their consumption by suitable electron acceptors and donors should occur at the same time. Otherwise, the generation of the e_{cb}^-−h_{vb}^+ pair would be inhibited, and the photocatalytic reaction would be terminated. In other words, none of Bi_2WO_6 and WO_3 is expected to be active for the photocatalytic degradation of organic pollutants in an aerated aqueous solution. This expectation has been confirmed with WO_3, but not with Bi_2WO_6, as cited above. It is highly possible that the reduction of O_2 by e_{cb}^- on Bi_2WO_6 is a multielectron process, different from that occurring on WO_3. Moreover, the reactive species responsible for the observed organic degradation over Bi_2WO_6 have been rarely studied.[18,20] Because O_2 is a green and resourceful oxidant, clarification of those questions is very

Received: October 15, 2013
Revised: January 15, 2014
Published: January 22, 2014

   dx.doi.org/10.1021/cs400927w | ACS Catal. 2014, 4, 732−737

important to further development of a visible-light-driven photocatalyst.

In this work, we report, for the first time, that the irradiated Bi_2WO_6 is not only active for water oxidation to $^{\bullet}OH$ but also active for the two-electron reduction of O_2 to produce H_2O_2. The flower-like Bi_2WO_6 was chosen as a representative of Bi_2WO_6, because it has a surface area as high as 42 m^2/g,[13] and shows a higher photocatalytic activity than 2D plate-like Bi_2WO_6 for RhB photodegradation.[19] To minimize the effect of dye sensitization and organic adsorption on the activity assessment, phenol was used as a model substrate, because it is colorless and hardly adsorbs on Bi_2WO_6 in aqueous suspension. Possible formation of H_2O_2 and $^{\bullet}OH$ radicals over the irradiated catalysts were examined by a colorimetric method, and 5,5-dimethyl-1-pyrroline-N-oxide (DMPO) spin trapping EPR, respectively. The flat band potential for the Bi_2WO_6 film electrode in aqueous solution was determined through the Mott−Schottky plot. Finally, a possible mechanism for the observed photoreactivity of Bi_2WO_6 is proposed.

EXPERIMENTAL SECTION

Materials. Chemicals were mostly purchased from Shanghai Chemicals, Inc., including $Na_2WO_4{\cdot}2H_2O$, $Bi(NO_3)_3{\cdot}5H_2O$, WO_3, phenol, H_2O_2, and polyvinylalcohol (PVA). Horseradish peroxide (POD), *N*,*N*-diethyl-*p*-phenylenediamine (DPD), H_2PtCl_6, and DMPO were purchased from Sigma-Aldrich, and catalase (CAT) from TCI, and PBS (phosphate-buffered saline) from Hangzhou Keyi Bio. Tech. Inc., China. Deionized and doubly distilled water was used throughout this study.

Synthesis. Flower-like Bi_2WO_6 was synthesized by a modified hydrothermal method.[12,13] Typically, $Na_2WO_4{\cdot}2H_2O$ (1.24 g) dissolved in water (40 mL) was added dropwise to the solution containing $Bi(NO_3){\cdot}5H_2O$ (3.64 g) and 0.4 M HNO_3 (30 mL). After sonication for 30 min, the suspension was transferred into a 150 mL Teflon-lined autoclave, and heated at 160 °C for 20 h. After the solution cooled to room temperature, the solid was collected by centrifugation, washed thoroughly with water, and dried at 80 °C. Then, the sample was sintered in air at 350 °C for 3 h.

Platinization of Bi_2WO_6 and WO_3, denoted as Pt−Bi_2WO_6 and Pt−WO_3, was carried out by following a photochemical deposition method.[5] The aqueous suspension (50 mL) containing CH_3OH (4 mL), H_2PtCl_6 (9.6 mg), and catalyst (0.90 g) was irradiated with a 300 W mercury lamp for 3 h. After that, the solid was collected by centrifugation, and thorough washing with water and ethanol. Finally, the black sample was dried at 80 °C overnight.

Characterization. X-ray diffraction (XRD) patterns were recorded on a D/max-2550/PC diffractometer (Rigaku). Raman spectra were obtained on a Jobin Yvon Lab Ram 1B with 632.8 nm He−Ne laser excitation. Adsorption isotherms of N_2 on solid were measured at 77 K on a Micromeritics ASAP2020 apparatus, from which the Brunauer−Emmett−Teller (BET) surface area was calculated. Diffuse reflectance spectra were recorded on a Varian Carry 500 using $BaSO_4$ as a reference. Scanning electron microscopy (SEM) was performed on a Hitachi S-4800. X-ray photoelectron spectroscopy (XPS) was performed with a Kratos AXIS UItra DLD spectrometer. The spectra were calibrated with C 1s at 284.8 eV. Element analysis was made on an inductive coupling plasma−mass spectroscopy (ICP-MS) on a Thermo Fisher X Series II instrument.

Photocatalysis and Analysis. The visible light source was a Xe-lamp (150 W) equipped with a 400 nm cutoff filter. The reactor was made of a Pyrex glass, and thermostatted at 25 °C through a water-cycling jacket. The light intensity reaching the external surface of the reactor was 25.2 mW/cm^2, as measured with an irradiance meter (Instruments of Beijing Normal University). The suspension (50 mL) containing necessary components (1.30 g/L catalyst, and 0.43 mM phenol) was first stirred in dark for 1 h, and then irradiated with visible light. At given intervals, small aliquots were taken, filtered (0.22 μm), and analyzed on a Dionex P680 HPLC (high performance liquid chromatography), equipped with an Apollo C18 reverse column. When necessary, H_2O_2 (12 mM) was added to the suspension just before light irradiation.

The solution absorption spectrum was recorded by using a 1 cm quartz cell on an Agilent 8453 UV−visible spectrophotometer. Hydrogen peroxide was analyzed at 551 nm through the POD-catalyzed oxidation of DPD.[21] Hydroxyl radicals were determined by a DMPO spin-trapping EPR method at room temperature on a Bruker ER200-D-SRC spectrometer at X-band, equipped with a Xenon lamp (100 W). Experiment was performed with a capillary Pyrex glass tube under fixed conditions (1.3 g/L catalyst, and 180 mM DMPO), and the EPR spectra were recorded at given intervals of light irradiation. In some experiments, CAT (300 U/mL) was also added for the catalytic removal of H_2O_2.[22]

Electrochemistry. Measurements were conducted with a three electrode cell with a quartz window, using a saturated calomel electrode (SCE) as reference electrode and a platinum wire as counter electrode. The electrolyte was 0.5 M $NaClO_4$, and the solution pH was adjusted with NaOH. The Bi_2WO_6 film was prepared on ITO glass by the doctor blade method, followed by annealing at 400 °C for 3 h. The film was weld with copper conducting paste for a better electrical contact, with a working surface area of 1.0 × 1.0 cm. The Mott−Schottky plot was obtained through measurement of the capacitance as a function of potentials at 3 kHz.[23,24]

RESULT AND DISCUSSION

The primary experiment for phenol degradation in water under visible light showed that the sample sintered at 350 °C was more active than the as-prepared Bi_2WO_6. Therefore, in this study, only the thermally treated sample will be examined as a photocatalyst. The SEM image, XRD pattern, N_2 adsorption isotherm, Raman, and diffuse reflectance spectra of flower-like Bi_2WO_6 are summarized in Figure S1 of the Supporting Information. Briefly, the solid had a spherical superstructure constructed from a number of nanoplates. It showed an XRD pattern typical of pure orthorhombic Bi_2WO_6 (PDF no. 39-0256). By using the Scherrer equation, the average crystallite size of Bi_2WO_6 along the (131) direction was calculated to be 17.9 nm. The solid had a BET surface area of 11.9 m^2/g, which was lower than that measured for the as-prepared Bi_2WO_6 (23.3 m^2/g), but larger than that measured with WO_3 (6.6 m^2/g). In the Raman spectrum, a set of vibrations was also in good agreement with those reported for Bi_2WO_6.[25,26] Moreover, in the UV−visible absorption spectrum, there was a broad absorption band at 200−450 nm, ascribed to the charge transfer from O^{2-} to W^{6+}. By using a derivative method,[27] the band gap energy of Bi_2WO_6 was estimated to be 2.82 eV, similar to those reported.[11−19]

The platinized Bi_2WO_6 and WO_3 were black in color, indicative of Pt particles successfully deposited onto the solid.

dx.doi.org/10.1021/cs400927w | ACS Catal. 2014, 4, 732−737

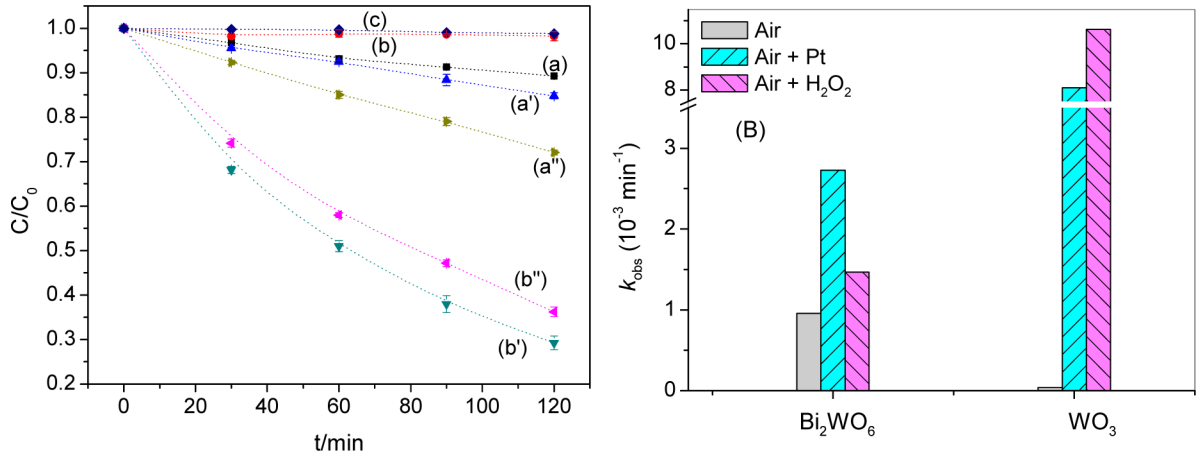

Figure 1. Phenol degradation under visible light in the aerated aqueous suspensions of (a) Bi_2WO_6, (b) WO_3, (a′) Bi_2WO_6 + H_2O_2, (b′) WO_3 + H_2O_2, (a″) Pt−Bi_2WO_6, (b″) Pt−WO_3, and (c) H_2O_2.

Element analysis by ICP-MS showed that the amounts of Pt present in Pt−Bi_2WO_6 and Pt-WO_3 were 0.30 and 0.29 wt %, respectively. Chemical state analysis by XPS showed that the binding energies of Pt $4f_{7/2}$ and Pt $4f_{5/2}$ were 70.9 and 74.3 eV for Pt−Bi_2WO_6, and 71.3 and 74.5 eV for Pt-WO_3, respectively. These binding energies are in agreement with those reported for the metallic Pt (70.7−71.6 eV for Pt $4f_{7/2}$, and 74.0−74.5 eV for Pt $4f_{5/2}$).[28,29]

Figure 1A shows the results of phenol degradation, obtained with different catalysts under visible light at wavelengths longer than 400 nm. First of all, in aerated aqueous solution, phenol degradation was observed with Bi_2WO_6, not with WO_3. Control experiments in the dark or under light irradiation in the absence of catalyst showed negligible phenol degradation. These observations confirm that for organic degradation in aerated aqueous solution, Bi_2WO_6 and WO_3 are good and poor photocatalysts, respectively.[4−10] Moreover, the time profile of phenol degradation over Bi_2WO_6 was satisfactorily fitted with the pseudo-first-order rate equation. A separate experiment in the N_2 purged aqueous suspension of Bi_2WO_6 under visible light showed negligible phenol degradation. This result clearly indicates that O_2 is required for phenol degradation, and that O_2 can react with the photogenerated e_{cb}^- on Bi_2WO_6, but not on WO_3 (eqs 1−3). Once O_2 is consumed for phenol degradation, it would be immediately supplied from air. As a result, the rate equation for phenol degradation on Bi_2WO_6 is first-order in phenol. Note that the kinetics of organic degradation on a semiconductor photocatalyst such as TiO_2 is a complicated issue,[1] and the detailed discussion about it is out of the present study.

$$e^- + O_2 + H^+ \rightarrow HO_2^\bullet \quad (1)$$

$$e^- + HO_2^\bullet + H^+ \rightarrow H_2O_2 \quad (2)$$

$$2e^- + O_2 + 2H^+ \rightarrow H_2O_2 \quad (3)$$

$$e^- + H_2O_2 + H^+ \rightarrow {}^\bullet OH + H_2O \quad (4)$$

Second, upon the addition of excess H_2O_2 (12 mM), phenol degradation on Bi_2WO_6 and WO_3 became fast (curves a′ and b′, Figure 1A). Control experiments in the dark or in the absence of catalyst under light irradiation showed negligible phenol degradation. This positive effect of H_2O_2 is in agreement with the fact that H_2O_2 is a stronger one-electron oxidant than O_2 [eq 4, E^o (H_2O_2/$^\bullet$OH) = 0.71 V vs NHE].[6] Third, after Bi_2WO_6 and WO_3 were loaded with 0.3 wt % Pt, phenol degradation also became fast (curves a″ and b″, Figure 1A), in relative to those in the absence of Pt. This is generally ascribed to noble metals that have a catalytic effect on the multiple electron reduction of O_2 [eq 3, E^o (O_2/H_2O_2 = 0.70 V vs NHE]).[5] Forth, in the presence of H_2O_2 or Pt, phenol degradation on Bi_2WO_6 and WO_3 all followed the first-order kinetics. The resulting apparent rate constants for phenol degradation are tabulated in Figure 1B. We see that in the presence of H_2O_2 or Pt, WO_3 is a better photocatalyst than Bi_2WO_6. In other words, WO_3 has a higher intrinsic photocatalytic activity than Bi_2WO_6. In the absence of additive, the poor activity of WO_3 is due to its e_{cb}^- being incapable of O_2 reduction.[6] Fifth, the chemical oxygen demand (COD) was measured by a chromate method. After 2 h of phenol degradation, the percentages of COD removal obtained with Bi_2WO_6, Pt/Bi_2WO_6 and Pt/WO_3 were 23.2, 29.0 and 21.5%, respectively. This observation indicates that phenol not only degrades but also undergoes mineralization, as reported with Bi_2WO_6 in the literature.[15]

Interestingly, the catalysts showed different behaviors toward H_2O_2 and Pt. With WO_3, the rate of phenol degradation increased in the order of H_2O_2 > Pt ≫ O_2, whereas with Bi_2WO_6, the rate of phenol degradation increased in another order of Pt > H_2O_2 > O_2. This observation indicates that H_2O_2 has a small effect on the Bi_2WO_6-photocatalyzed reaction, as compared to its large effect on the WO_3-photocatalyzed reaction. Recall that the one-electron reduction of O_2 on Bi_2WO_6 and WO_3 is not allowed in thermodynamics, but O_2 can react with the photogenerated e_{cb}^- on Bi_2WO_6 for phenol degradation (Figure 1A). Assume that the reduction of O_2 over Bi_2WO_6 is a two-electron transfer process (eq 3), then the different effects of H_2O_2 observed with Bi_2WO_6 and WO_3 is explainable. It is known that the reduction of H_2O_2 to $^\bullet$OH and the reduction of O_2 to H_2O_2 have similar standard redox potentials (see above). Then, O_2 would compete with H_2O_2 for e_{cb}^- on Bi_2WO_6. As a result, H_2O_2 only shows a small effect on the Bi_2WO_6-photocatalyzed reaction. On the contrary, WO_3 had a negligible activity for phenol degradation in aerated aqueous suspension, due to its e_{cb}^- is not removable by O_2 through one-electron pathway. Therefore, H_2O_2 shows a large effect on the WO_3-photocatalyzed reactions. In the presence of Pt, the multielectron reduction of O_2 to H_2O_2 on each catalyst

dx.doi.org/10.1021/cs400927w | ACS Catal. 2014, 4, 732−737

is catalytically accelerated. Because e_{cb}^- and h_{vb}^+ are generated in a pair, this would result into great improvement in the efficiency of charge separation, and consequently in the rate of phenol degradation. Furthermore, in the presence of H_2O_2 or Pt, phenol degradation on WO_3 was much faster than that on Bi_2WO_6. This observation suggests that WO_3 has a higher intrinsic photocatalytic activity than Bi_2WO_6, as its e_{cb}^- is efficiently removed by O_2 or by H_2O_2 (eqs 3 or 4).

To provide evidence for the multielectron reduction of O_2, the possible formation of H_2O_2 was examined by a colorimetric DPD method.[21] The experiment was carried out in the presence of phenol in the aerated aqueous suspensions of catalysts under visible light, and the result is shown in Figure 2.

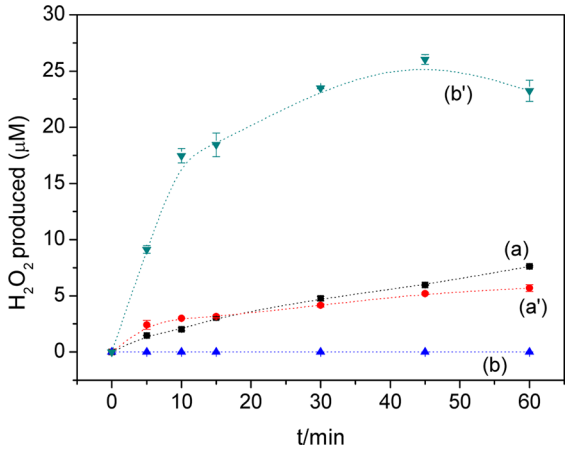

Figure 2. Production of H_2O_2 under visible light in the aerated aqueous suspensions of (a) Bi_2WO_6, (b) WO_3, (a′) Pt−Bi_2WO_6, and (b′) Pt−WO_3, in the presence of phenol.

With WO_3, the photogeneration of H_2O_2 was very slow or negligible, but it became rather fast in the presence of Pt. This result is in agreement with the previous conclusion that Pt particles deposited on WO_3 can catalyze the two-electron reduction of O_2 to form H_2O_2.[5] Surprisingly, in the irradiated aerated aqueous solution of Bi_2WO_6, the production of H_2O_2 was very obvious. This new observation gives a strong support of the above hypothesis that the reduction of O_2 over Bi_2WO_6 is a two-electron transfer process (eq 3). However, the Pt-catalyzed production of H_2O_2 on Bi_2WO_6 was not significant, as compared to that on WO_3. This discrepancy in the rate enhancement of H_2O_2 production between the catalysts might be due to three factors. First, it is known that Pt particles also have a catalytic effect on the decomposition of H_2O_2 (eq 5).[5] Then, there would be a competition between the Pt-catalyzed generation and decomposition of H_2O_2. As a result, with each catalyst, the concentration of H_2O_2 appeared to increase toward saturation and/or decline as irradiation time increased. Second, the rate of photocatalytic reaction is primarily determined by the rate of e_{cb}^-−h_{vb}^+ production. Because Bi_2WO_6 has a lower intrinsic photoactivity than WO_3, it shows a slower production of H_2O_2 than WO_3 in the presence of Pt. Third, the two-electron reduction of O_2 on Bi_2WO_6 can occur even in the absence of Pt. Therefore, the noble metal only shows a small effect on the production of H_2O_2 on Bi_2WO_6, in relative to that on WO_3.

$$2H_2O_2 \rightarrow O_2 + 2H_2O \quad (5)$$

Possible involvement of $^\bullet$OH radicals in the reaction was then examined by using a DMPO spin-trapping EPR technique. Figure 3A shows the EPR spectrum obtained with Bi_2WO_6 in an aerated aqueous suspension in the absence of phenol. In the dark, there was no EPR signal. After illumination with UV light, a quartet signal characteristic of the DMPO−$^\bullet$OH adduct was observed. Note that under visible light, the EPR signal was rather weak.[18] Because the EPR signal was time-dependent, the results obtained with different catalysts were then compared under similar conditions. In all cases, the signal intensity did not linearly increase with the increase of irradiation time (Figure 3B). This observation is due to DMPO concentration that decreases with the time, and due to the degradation of DMPO by $^\bullet$OH,[30] and/or due to the slow degradation of DMPO−$^\bullet$OH in the dark.[31] However, according to the initial rate of the adduct formation, the catalyst activity could be concluded in the increasing order of Pt-WO_3 > Pt−Bi_2WO_6 > Bi_2WO_6 > WO_3. This trend in the rate of $^\bullet$OH generation among the catalysts is in agreement with those in the rates of phenol degradation and H_2O_2 production (Figures 1 and 2). Note that with Pt−Bi_2WO_6, the signal after reaching a maximum becomes obviously to decrease with the irradiation time (curve c, Figure 3B). Because Pt has a catalytic effect on the decomposition of H_2O_2, this observation probably indicates that H_2O_2 is involved in the production of $^\bullet$OH radicals (eq 4).

$$h_{vb}^+ + H_2O \text{ (or } OH^-) \rightarrow {}^\bullet OH + H^+ \quad (6)$$

In general, $^\bullet$OH radicals can result from the reductive path (eq 4), from the oxidative path (eq 6), and/or from both.[1−3] To verify the source for $^\bullet$OH production, H_2O_2 was removed by using CAT as a catalyst.[22] Figure 3C shows the time profiles of signal intensity measured in the absence and presence of CAT. Note that a phosphate buffer (PBS) is needed for stabilization of biological reagent CAT. First of all, in the presence of PBS, the signal intensity of the DMPO−$^\bullet$OH adduct was reduced, probably due to the PBS-induced aggregation of Bi_2WO_6 particles (curves a and a′, Figure 3C). Second, in the presence of both PBS and CAT (300 U/mL), the signal intensity was further reduced, but not completely disappeared (curve a″, Figure 3C). Such signal remained unchanged with excess CAT (3000 U/mL). This observation indicates that H_2O_2 has been completely removed by CAT, and that the production of $^\bullet$OH over the irradiated Bi_2WO_6 in an aerated aqueous suspension can occur through both the reductive and oxidative pathways (eqs 4 and 6).

By means of the Mott−Schottky plot (Figure S2, Supporting Information),[23,24] the flat band potential for the Bi_2WO_6 film electrode was determined to be +0.25 V vs NHE at pH 0. This potential for the flower-like Bi_2WO_6 is close to that measured recently for the leaf-like Bi_2WO_6 (+0.31 V vs NHE at pH 0),[16] but it is more negative than that for WO_3 used in the present study (+0.45 V vs NHE at pH 0).[7] For an *n*-type semiconductor, the flat band potential is close to the conduction band potential. According to the band gap energies of Bi_2WO_6 (2.82 eV) and WO_3 (2.6 eV), their valence band potentials are approximately 3.0 V vs NHE at pH 0, which is more positive than that for the $H_2O/^\bullet OH$ couple (E° = +2.80 V vs NHE). Therefore, water oxidation to $^\bullet$OH radical by h_{vb}^+ on Bi_2WO_6 and WO_3 are both thermodynamically plausible (eq 6), as observed by EPR in Figure 3C. On the other hand, the flat band potentials of Bi_2WO_6 and WO_3 are more positive than the one-electron reduction potential of O_2. This would do not allow the one-electron reduction of O_2 to occur either with

dx.doi.org/10.1021/cs400927w | ACS Catal. 2014, 4, 732−737

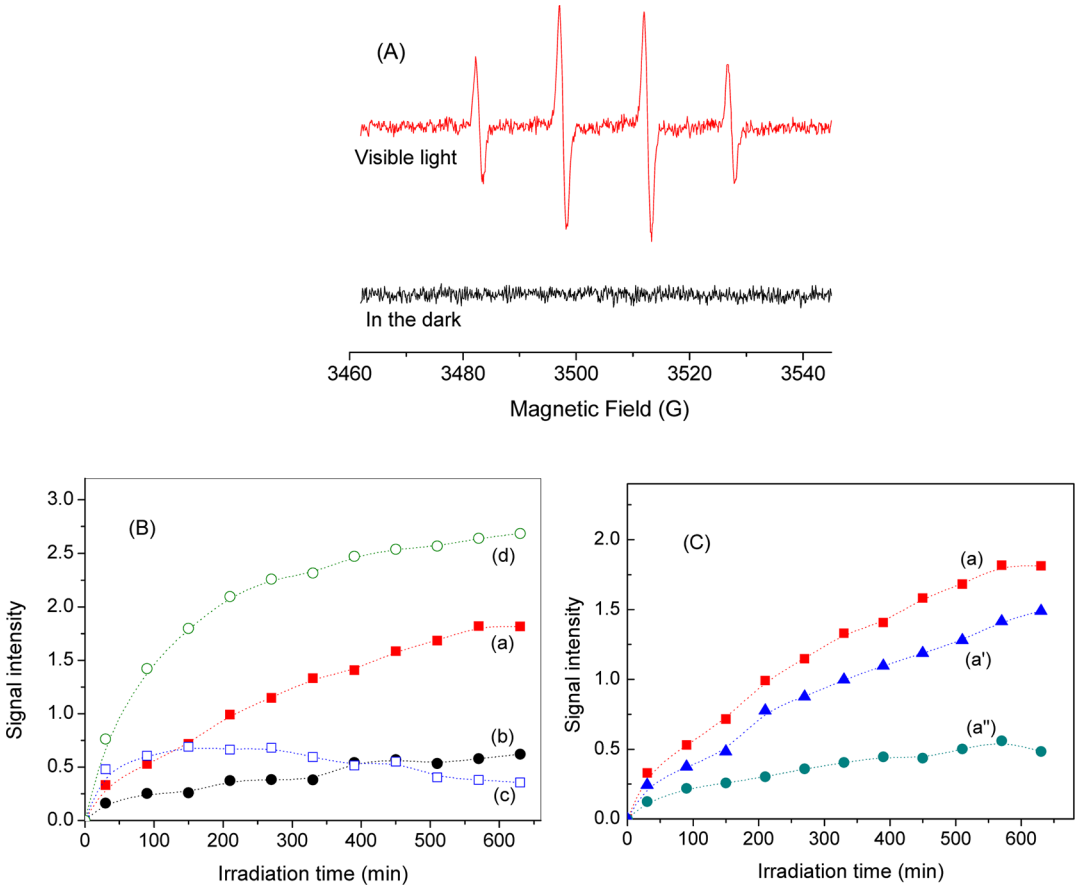

Figure 3. (A) EPR spectra of the DMPO−•OH adducts, recorded with Bi_2WO_6 in the dark and after UV light in the absence of phenol. (B) The second peak intensity obtained with (a) Bi_2WO_6, (b) WO_3, (c) Pt−Bi_2WO_6, and (d) Pt−WO_3, and (C) The second peak intensity obtained with Bi_2WO_6 in the presence of (a′) PBS and (a″) CAT containing PBS.

Bi_2WO_6 or WO_3. However, the two-electron reduction of O_2 to form H_2O_2 can occur with Bi_2WO_6, whereas such reaction occurring on WO_3 needs the noble metal of Pt as a thermal catalyst.[5]

CONCLUSION

In this work, we have proposed that the observed organic degradation over the irradiated Bi_2WO_6 in aerated aqueous solution is due to the production of •OH and H_2O_2. Although the valence hole of WO_3 is also capable of water oxidation to •OH, its conduction band electron is not reactive toward O_2 through either one- or two-electron pathway. This proposal is supported by several evidence, including the effects of H_2O_2 and Pt, and the in situ measurement of H_2O_2 and •OH radicals. According to our knowledge, there are few photocatalysts capable of the multielectron reduction of O_2. In this regard, flower-like Bi_2WO_6 is good, because it is active under both UV and visible light. However, the two-electron reduction of O_2 is usually slower than the one-electron reduction of O_2, which would limit application of Bi_2WO_6 for environmental use. Further effort is needed for improvement of the catalyst photocatalytic activity of Bi_2WO_6.

ASSOCIATED CONTENT

Supporting Information

XRD pattern, N_2 adsorption−desorption isotherms, Raman, diffuse reflectance, and Mott−Schottky plots. This material is available free of charge via the Internet at http://pubs.acs.org.

AUTHOR INFORMATION

Corresponding Author

*Y. Xu. E-mail: xuym@css.zju.edu.cn. Fax: +86-571-87951895. Tel: +86-571-87952410.

Notes

The authors declare no competing financial interest.

ACKNOWLEDGMENTS

This work was supported by the 973 program of China (Nos. 2009CB825300, and 2011CB936003). We thank Dr. Wenhua Leng and Run Liu for their kind help in solid spectra and electrochemical measurement.

REFERENCES

(1) Hoffmann, M. R.; Martin, S. T.; Choi, W.; Bahnemann, D. W. *Chem. Rev.* **1995**, *95*, 69−96.
(2) Carp, O.; Huisman, C. L.; Reller, A. *Solid State Chem.* **2004**, *32*, 33−177.
(3) Tachikawa, T.; Fujitsuka, M.; Majima, T. *J. Phys. Chem. C* **2007**, *111*, 5259−5275.
(4) Abe, R.; Takami, H.; Murakami, N.; Ohtani, B. *J. Am. Chem. Soc.* **2008**, *130*, 7780−7781.
(5) Kim, J.; Lee, C. W.; Choi, W. *Environ. Sci. Technol.* **2010**, *44*, 6849−6857.
(6) Bi, D.; Xu, Y. *Langmuir* **2011**, *27*, 9359−9366.
(7) Bi, D.; Xu, Y. *J. Mol. Catal. A: Chem.* **2013**, *367*, 103−107.
(8) Nenadović, M. T.; Rajh, T.; Mićić, O. I.; Nozik, A. J. *J. Phys. Chem.* **1984**, *88*, 5827−5830.

(9) Zhang, L.; Wang, H.; Chen, Z.; Wong, P. K.; Liu, J. *Appl. Catal., B* **2011**, *106*, 1−13.
(10) Zhang, L.; Zhu, Y. *Catal. Sci. Technol.* **2012**, *2*, 694−706.
(11) Kudo, A.; Hijii, S. *Chem. Lett.* **1999**, *10*, 1103−1104.
(12) Amano, F.; Nogami, K.; Abe, R.; Ohtani, B. *J. Phys. Chem. C* **2008**, *112*, 9320−9326.
(13) Zhang, L.; Wang, W.; Chen, Z.; Zhou, L.; Xu, H.; Zhu, W. *J. Mater. Chem.* **2007**, *17*, 2526−2532.
(14) Amano, F.; Yamakata, A.; Nogami, K.; Osawa, M.; Ohtani, B. *J. Phys. Chem. C* **2011**, *115*, 16598−16605.
(15) Sun, S.; Wang, W.; Zhang, L. *J. Phys. Chem. C* **2012**, *116*, 19413−19418.
(16) Gao, E.; Wang, W.; Shang, M.; Xu, J. *Phys. Chem. Chem. Phys.* **2011**, *13*, 2887−2893.
(17) Xu, Q. C.; Wellia, D. V.; Ng, Y. H.; Amal, R.; Tan, T. T. Y. *J. Phys. Chem. C.* **2011**, *115*, 7419−7428.
(18) Fu, H.; Pan, C.; Yao, W.; Zhu, Y. *J. Phys. Chem. B* **2005**, *109*, 22432−22439.
(19) Zhang, L.; Wang, W.; Zhou, L.; Xu, H. *Small* **2007**, *3*, 1618−1625.
(20) Wang, C.; Zhang, H.; Li, F.; Zhu, L. *Environ. Sci. Technol.* **2010**, *44*, 6843−6848.
(21) Bader, H.; Sturzenegger, V.; Hoigné, J. *Water Res.* **1988**, *22*, 1109−1115.
(22) Khachatryan, L.; Vejerano, E.; Lomnicki, S.; Dellinger, B. *Environ. Sci. Technol.* **2011**, *45*, 8559−8566.
(23) Kavan, L.; Grätzel, M.; Gilbert, S. E.; Klemenz, H. J. *J. Am. Chem. Soc.* **1996**, *118*, 6716−16723.
(24) Cooper, G.; Turner, A. J.; Nozik, A. J. *J. Electrochem. Soc.* **1982**, *129*, 1973−11977.
(25) Maczka, M.; Macalik, L.; Hermanowicz, K.; Kepiński, L.; Tomaszewski, P. *J. Raman Spectrosc.* **2010**, *41*, 1059−1066.
(26) Graves, P. R.; Hua, G.; Myhra, S.; Thompson, J. G. *J. Solid State Chem.* **1995**, *114*, 112−1122.
(27) Chakrabarti, S.; Ganguli, D.; Chaudhuri, S. *Phys. E (Amsterdam, Neth.)* **2004**, *24*, 333−342.
(28) Bera, P.; Priolkar, K. R.; Gayen, A.; Sarode, P. R.; Hegde, M. S.; Emura, S.; Kumashira, R.; Jayaram, V.; Subbanna, G. N. *Chem. Mater.* **2003**, *15*, 2049−2060.
(29) Arico, A. S.; Shukla, A. K.; Kim, H.; Park, S.; Min, M.; Antonucci, V. *Appl. Surf. Sci.* **2001**, *172*, 33−40.
(30) Watanabe, N.; Horikoshi, S.; Hidaka, H.; Serpone, N. *J. Photochem. Photobiol. A* **2005**, *174*, 229−238.
(31) Grela, M. A.; Coronel, M. E. J.; Colussi, A. J. *J. Phys. Chem.* **1996**, *100*, 16940−16946.